Soliton breathers in spin-1 Bose–Einstein condensates*

Ji Shen-Tong(冀慎统), Yan Pei-Gen(颜培根), and Liu Xue-Shen(刘学深)†

Institute of Atomic and Molecular Physics, Jilin University, Changchun 130012, *China*

(Received 27 September 2013; revised manuscript received 7 November 2013; published online 24 January 2014)

We consider a spin-1 Bose–Einstein condensate trapped in a harmonic potential with different nonlinearity coefficients. We illustrate the dynamics of soliton breathers in two-component and three-component states by numerically solving the one-dimensional time-dependent coupled Gross–Pitaecskii equations (GPEs). We present that two condensates with repulsive interspecies interactions make elastic collision and novel soliton breathers are created in two-component state. We also demonstrate novel soliton breathers in three-component state with attractive coupling constants. Furthermore, possible reasons for creating soliton breathers are discussed.

Keywords: spin-1 Bose–Einstein condensate, soliton breathers, Gross–Pitaecskii equations (GPEs)

PACS: 03.75.Mn, 03.75.Lm, 03.75.Kk **DOI:** 10.1088/1674-1056/23/3/030311

1. Introduction

Spinor Bose–Einstein condensates (BECs) have internal degree of freedom due to the hyperfine spin of atoms. When spinor BECs are trapped in magnetic potential, the spin degree of freedom is frozen. While when spinor BECs are trapped in optical potential, the spin degree of freedom comes into play. Since they were first observed by MIT group[1] in optical potentials, many interesting phenomena in spinor BECs that are not presented in single-component systems has been observed, such as the formation of spin domains[2] and spin-mixing dynamics,[3] coreless vortices,[4,5] and skyrmions.[6,7]

A spinor condensate formed by atoms with spin 1 is described by a macroscopic wave function $\boldsymbol{\Psi} = (\Psi_{+1}, \Psi_0, \Psi_{-1})^{\mathrm{T}}$ with three components. Under a special constraint on the condensate parameters, the three-component nonlinear equations can be reduced to an integrable model which supports soliton solution. Hence, great efforts have been made to understand macroscopic nonlinear structures in spinor BECs, such as bright solitons,[8–10] dark solitons,[11] dark–bright solitons,[12] and gap solitons.[13] In addition, there is a particle collision process in a spin-1 BEC which holds the conservation of total spins: two atoms with spin components Ψ_{+1} and Ψ_{-1} can scatter into final states containing two atoms with spin component Ψ_0 upon an elastic collision, and vice versa. This process is coherent so that it leads to oscillations of spin population and also helps to support the existence of spinor solitons.

Solitons are a nonlinear effect that arises when the nonlinearity and the dispersion cancel out each other. Solitons are characterized by localized solitary wave packets that maintain their shape and amplitude while propagating. Solitons can also periodically change the width and the peak maximum, in which case they are known as the soliton breathers.[14,15] In the BEC context, the condensates of weakly interacting atoms can be described by the Gross–Pitaevskii (GP) equation or the nonlinear Schrödinger equation, and it can be used in the study of solitons and collapse. As is known to all, when the condensates are trapped in a harmonic potential, stable solitons exist in a finite range of the scattering length. Outside that range (e.g., when the attractive particle interactions are too strong), the condensates collapse, while the condensates without the trap potential can dissolve when the interactions are weakly attractive.

Feshbach resonance[16–18] is an effective mechanism that can be used to manipulate the sign and the magnitude of scattering length, which has been widely used in experimental studies, such as the formation of rogue waves,[15,19] bright solitons,[20,21] bright and dark soliton trains,[22] spontaneous symmetry breaking of a Bose–Fermi mixture[23,24] or spinor BECs.[25] After the scattering length has periodic changes of the magnitude and/or sign via the Feshbach resonance, novel bright matter-wave breathers are created in single-component BECs[26] and two-component BECs.[27]

In this paper, we present stable soliton breathers of spin-1 condensates in a harmonic trap potential by tuning nonlinear interactions. The dynamics of soliton breather solutions in spinor Bose–Einstein condensates is studied by numerically solving the one-dimensional (1D) time-dependent coupled GPEs. In particular, we aim to analyze the dynamics of soliton breathers in two-component and three-component cases.

The paper is organized as follows. In Section 2, we introduce the theoretical model of spin-1 condensates in a harmonic trap potential. In Section 3, we illustrate the numerical results for the soliton breather in each state by tuning nonlinear interactions. Our conclusions are given in Section 4.

*Project supported by the National Natural Science Foundation of China (Grant Nos. 11271158 and 11174108).

†Corresponding author. E-mail: liuxs@jlu.edu.cn

© 2014 Chinese Physical Society and IOP Publishing Ltd

2. Model

We consider a quasi-1D BEC of alkali atoms with hyperfine spin-1 loaded in a harmonic trapping potential. The assembly of atoms in condensates is described by vector order parameter $\boldsymbol{\Psi} = (\Psi_{+1}, \Psi_0, \Psi_{-1})^{\mathrm{T}}$ with the components subject to the hyperfine spin space, and the normalization condition is $\int \boldsymbol{\Psi}(x)^{\mathrm{T}} \boldsymbol{\Psi}(x)\, \mathrm{d}x = N$, where N is the total number of atoms. In the mean-field approximation, the condensates on a spin-1 BEC whose macroscopic wave function $\boldsymbol{\Psi}$ may be written as $\boldsymbol{\Psi} = \sqrt{N}\psi = \sqrt{N}(\psi_{+1}, \psi_0, \psi_{-1})^{\mathrm{T}}$, $\int \psi^{\mathrm{T}} \psi\, \mathrm{d}x = 1$. We introduce the relative densities $\rho_j = (\psi_j, \psi_j) = \int \psi_j^{\mathrm{T}} \psi_j\, \mathrm{d}x$. The ψ satisfy the following coupled GP equation:[28,29]

$$\begin{aligned} \mathrm{i}\hbar\partial_t \psi \;=\; & \Bigg[-\frac{\hbar^2}{2M}\partial_x^2 + V_{\mathrm{ext}} + NC_0 \psi^+ \psi \\ & + NC_2 \left(\sum_{\alpha=1}^{3} \psi^+ f^\alpha \psi \right) \Bigg] \psi. \end{aligned} \tag{1}$$

Here, M is the mass of each atom, $V_{\mathrm{ext}} = \mathrm{diag}(V_{+1}(x), V_0(x), V_{-1}(x))$ are harmonic and spin-independent trapping potentials. The $\boldsymbol{f}^\alpha\ (\alpha = 1,2,3)$ are spin-1 matrices, which are given by

$$\begin{aligned} \boldsymbol{f}^1 &= \frac{1}{\sqrt{2}} \begin{pmatrix} 0 & 1 & 0 \\ 1 & 0 & 1 \\ 0 & 1 & 0 \end{pmatrix}, \quad \boldsymbol{f}^2 = \frac{\mathrm{i}}{\sqrt{2}} \begin{pmatrix} 0 & -1 & 0 \\ 1 & 0 & -1 \\ 0 & 1 & 0 \end{pmatrix}, \\ \boldsymbol{f}^3 &= \begin{pmatrix} 1 & 0 & 0 \\ 0 & 0 & 0 \\ 0 & 0 & -1 \end{pmatrix}. \end{aligned} \tag{2}$$

The coefficients C_0 and C_2, which control the spin-independent and spin-dependent interactions, respectively, are

$$C_0 = \frac{2\hbar\omega_\perp(g_0 + 2g_2)}{3}, \quad C_2 = \frac{2\hbar\omega_\perp(g_2 - g_0)}{3}, \tag{3}$$

where $\omega_\perp$ corresponds to the transverse trap frequency, g_0 and g_2 are the s-wave scattering lengths corresponding to the total spin of the two colliding bosons 0 and 2, respectively.

We choose that time, length, and energy are measured in units of ω_x^{-1} (ω_x corresponds to the longitudinal trap frequency), $a_{\mathrm{s}} = \sqrt{\hbar/M\omega_x}$, and $\hbar\omega_x$, respectively.[30] This is equivalent to setting $\hbar = M = \omega_x = 1$, and the previous coupled GP equation (1) becomes

$$\mathrm{i}\partial_t \psi = \left[-\frac{1}{2}\partial_x^2 + V_{\mathrm{ext}} + c_0 \psi^\dagger \psi + c_2 \left(\sum_{\alpha=1}^{3} \psi^\dagger f^\alpha \psi \right) \right] \psi, \tag{4}$$

where we have introduced shorthand notation for the effective interaction coefficients, $c_0 = 2N\omega_\perp(g_0 + 2g_2)/3\omega_x a_{\mathrm{s}}$ and $c_2 = 2N\omega_\perp(g_2 - g_0)/3\omega_x a_{\mathrm{s}}$. We introduce the quantities $\langle x \rangle_j$ and $\langle R \rangle_j$ that describe the center-of-mass coordinate and the width of condensates in ψ_j component, which are defined as $\langle x \rangle_j = \int_{-\infty}^{\infty} \mathrm{d}x \left|\psi_j\right|^2 x/\rho_j$ and $\langle R \rangle_j^2 = \int_{-\infty}^{\infty} \mathrm{d}x \left|\psi_j\right|^2 \left(x - \langle x \rangle_j\right)^2$, respectively. We also introduce the quantity ΔX that describes the interval between centers of the condensates in components ψ_{+1} and ψ_{-1}, which is defined as $\Delta X = |\langle x \rangle_{+1} - \langle x \rangle_{-1}|$. Taking into account the simulation error, we replace $\langle x \rangle_j$ by the coordinate of the peak of soliton when the condensates form soliton.

Stationary states of system (4) can be classified into one-, two-, or three-component states.[31] We examine each case separately and find exact one-, two-, and three-component soliton solutions.

3. Numerical results

In our numerical simulations, we discretize the coupled GP equation (4) with time step $\Delta t = 0.001$ and space step $\Delta x = 0.025$. The ground state of condensates is obtained by propagating in imaginary time, and the evolution of condensates is obtained by time-splitting spectral method[32,33] starting from its ground state.

In this paper, we consider the system with the attractive coupling constants, i.e., $c_0 < 0$ and $c_2 < 0$. The effective interactions between atoms in BECs may be adjusted by means of the Feshbach resonance technique.

As is well known, soliton breather is created in one-component BECs when the nonlinearity coefficient is modulated periodically.[14,26] In the following paper, we focus on analyzing the two-component and three-component soliton solution.

3.1. Two-component solutions

We illustrate soliton's collision in two-component state (i.e., $\psi = (\psi_{+1}, 0, \psi_{-1})^{\mathrm{T}}$). We assume that the two components are initially loaded into two different traps, $V_j(x)$, of the same strength, centered at different positions, namely,

$$V_j(x) = \frac{1}{2}(x - jx_0)^2, \quad j = +1, -1. \tag{5}$$

The BECs fulfill the 1D GPEs as follows:

$$\begin{aligned} \mathrm{i}\partial_t \psi_{+1} \;=\; & \Bigg[-\frac{1}{2}\partial_x^2 + \frac{1}{2}(x - x_0)^2 + (c_0 + c_2)\left|\psi_{+1}\right|^2 \\ & + (c_0 - c_2)\left|\psi_{-1}\right|^2 \Bigg] \psi_{+1}, \\ \mathrm{i}\partial_t \psi_{-1} \;=\; & \Bigg[-\frac{1}{2}\partial_x^2 + \frac{1}{2}(x + x_0)^2 + (c_0 + c_2)\left|\psi_{-1}\right|^2 \\ & + (c_0 - c_2)\left|\psi_{+1}\right|^2 \Bigg] \psi_{-1}. \end{aligned} \tag{6}$$

Here, we choose $x_0 = 1$ and consider the BECs with three different scenarios: (a) $c_0 = c_2 = -1.0$, (b) $c_0 = -1.0$, $c_2 = -0.5$, and (c) $c_0 = -1.0$, $c_2 = -1.5$. These three scenarios can illustrate the effect of interspecies interaction on the collision of two condensates. In order to study this effect, we prepare the same ground states of these scenarios with $c_0 = c_2 = -1.0$ by using the imaginary time propagation method starting with the test wave function: $\psi_{+1}(x) = \psi_{-1}(x) = \pi^{-1/4} \exp\left(-x^2/2\right)$,

and take this ground state as an initial state of two-component condensates. The time evolution of the system (6) is obtained by the time-splitting spectral method starting from its initial state.

We first consider the situation of $c_0 = c_2 = -1.0$, in which the condensates in the components ψ_{+1} and ψ_{-1} can be regarded as two-species atomic BECs without interspecies interactions. After preparing the ground state, two traps ($V_{+1}(x)$ and $V_{-1}(x)$) are suddenly changed into $V_{\pm1}(x) = \frac{1}{2}x^2$. Under this condition, the time evolution of the two-component state is shown in Fig. 1.

Figure 1(b) shows the spatiotemporal contour plot of the density in the ψ_{+1} component. A bright soliton is created in ψ_{+1} component. It performs periodic oscillation at about $x = 0$, and the force acting on the soliton is $F = -x$. This bright soliton is similar to that illustrated in Ref. [34]. This verifies that when the condensates are trapped in a harmonic trap, stable solitons exist in a finite range of the scattering length.

As seen in Fig. 1(a), bright solitons propagate without changing their shapes after colliding with each other. In addition, the condensates in components ψ_{+1} and ψ_{-1} have the same peak densities (i.e., the same amplitudes). This phenomenon verifies that two solitons without interspecies interactions pass through one another. It is clear that soliton without interaction can propagate in its own way.

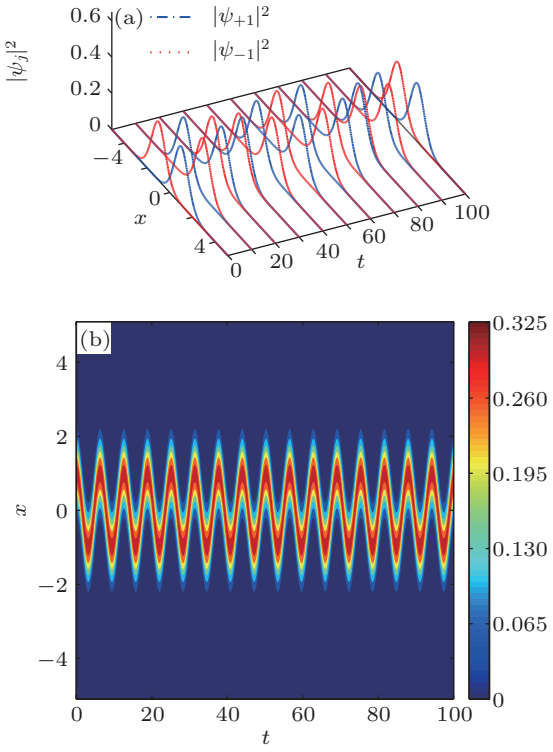


Fig. 1. (color online) Initialization of the system (6) is that the $\psi_{\pm1}$ components with nonlinearity coefficients $c_0 = c_2 = -1.0$ are loaded into two different traps $V_{\pm1}(x) = \frac{1}{2}(x \mp 1)^2$, respectively. Then the two traps $V_{\pm1}(x)$ are all suddenly changed into $V_{\pm1}(x) = \frac{1}{2}x^2$ at $t = 0$. (a) Time evolution of the densities $|\psi_{\pm1}(x,t)|^2$ in two components. (b) Spatiotemporal contour plot of the density, $|\psi_{+1}(x,t)|^2$. Here x, t, and $|\psi_j|^2 (j = +1, -1)$ are measured in units of a_s, ω_x^{-1}, and a_s^{-1}, respectively.

We then consider the situation of $c_0 = -1.0$ and $c_2 = -0.5$, in which the condensates in the components ψ_{+1} and ψ_{-1} can be regarded as two-species atomic BECs with attractive interspecies interactions. Using the same step as the first scenario, the time evolution of the two-component state is shown in Fig. 2.

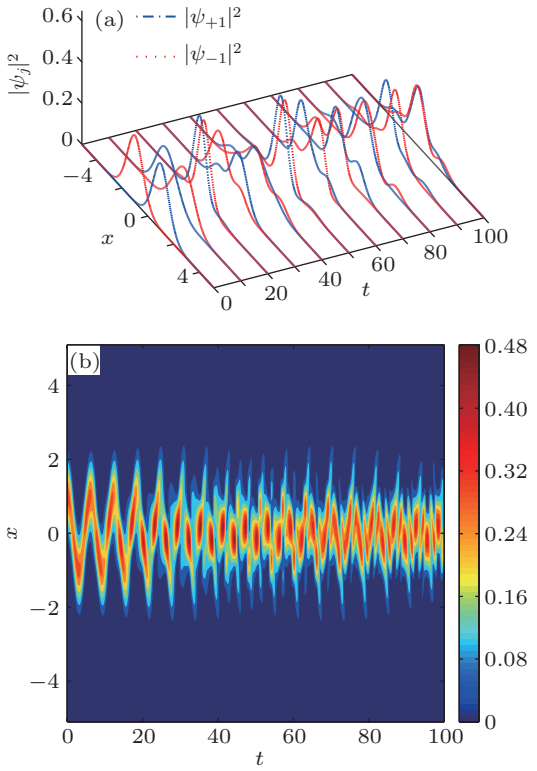


Fig. 2. (color online) Same situation as Fig. 1, but the nonlinearity coefficients $c_0 = -1.0$ and $c_2 = -0.5$. (a) Time evolution of the densities $|\psi_{\pm1}(x,t)|^2$ in two components. (b) Spatiotemporal contour plot of the density, $|\psi_{+1}(x,t)|^2$. Here x, t, and $|\psi_j|^2 (j = +1, -1)$ are measured in units of a_s, ω_x^{-1}, and a_s^{-1}, respectively.

Figure 2(b) shows the spatiotemporal contour plot of the density in the ψ_{+1} component. It is irregular, which indicates that this two-component state is unstable. As seen in Fig. 2(a), after the two traps are changed from $V_{\pm1}(x) = \frac{1}{2}(x \mp 1)^2$ into $V_{\pm1}(x) = \frac{1}{2}x^2$, the condensates in components ψ_{+1} and ψ_{-1} make inelastic collision for attractive interspecies interactions, and this collision leads to the asymmetric density profiles of the condensates in component ψ_{+1} (or ψ_{-1}) with respect to the position of its peak density. However, the ψ_{+1} and ψ_{-1} components are symmetric with respect to $x = 0$. In this situation, no soliton breather is created in ψ_{+1} (or ψ_{-1}) component.

Finally, we consider the situation of $c_0 = -1.0$ and $c_2 = -1.5$, in which the condensates in the components ψ_{+1} and ψ_{-1} can be regarded as two-species atomic BECs with repulsive interspecies interactions. Using the same step as the first scenario, novel soliton breathers are created in the $\psi_{\pm1}$ components, which are shown in Figs. 3(a) and 3(b).

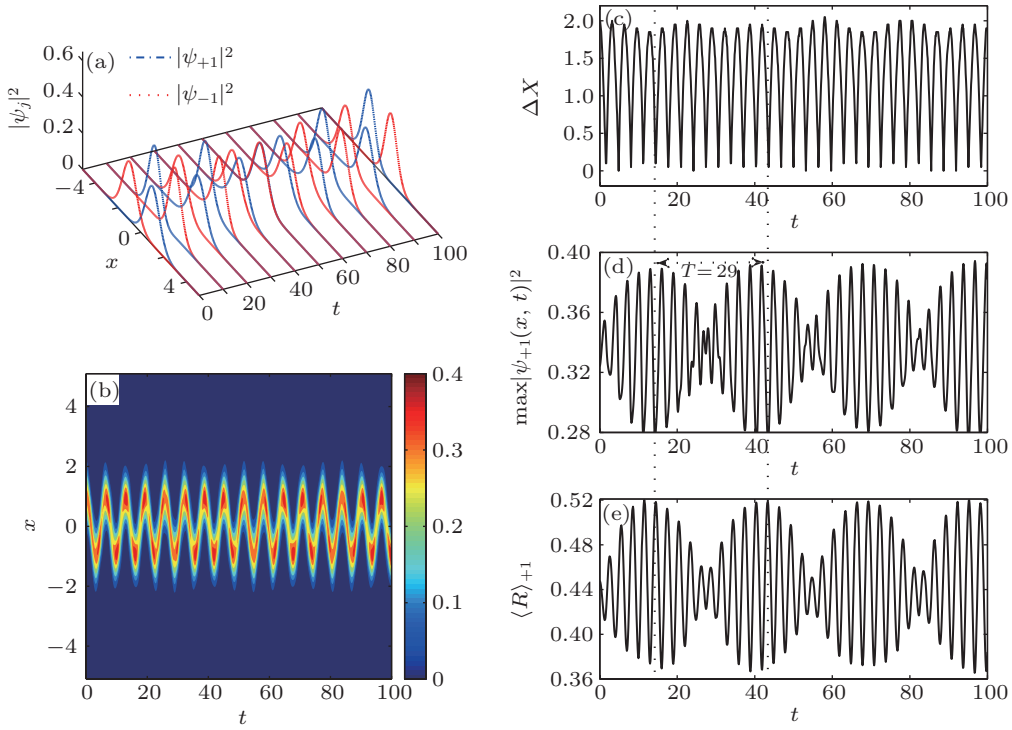


Fig. 3. (color online) Same situation as Fig. 1, but the nonlinearity coefficients $c_0 = -1.0$ and $c_2 = -1.5$. (a) Time evolution of the densities $|\psi_{\pm1}(x,t)|^2$ in two components. (b) Spatiotemporal contour plot of the density, $|\psi_{+1}(x,t)|^2$. (c), (d), and (e) Time evolution of ΔX (i.e., the interval between two solitons' centers in two components), the peak density $\max|\psi_{+1}(x,t)|^2$, and the width of soliton $\langle R\rangle_{+1}$ in ψ_{+1} component. Here x, ΔX, and $\langle R\rangle_{+1}$ are measured in units of a_s. The t and $|\psi_j|^2 (j = +1, -1)$ are measured in units of ω_x^{-1} and a_s^{-1}, respectively.

As seen in Fig. 3(a), after the two traps are changed from $V_{\pm1}(x) = \frac{1}{2}(x \mp 1)^2$ into $V_{\pm1}(x) = \frac{1}{2}x^2$ at $t = 0$, the condensates in components ψ_{+1} and ψ_{-1} make elastic collision. Figure 3(b) shows the spatiotemporal contour plot of the density in the ψ_{+1} component. From this figure, we can see that the condensates in the ψ_{+1} component perform periodic oscillation about $x = 0$, and the peak density of the condensates varies with time t. Moreover, due to the exist of harmonic trapping potential, the condensates are confined to a small region and do not dissolve. Thus, soliton is created in ψ_{+1} component, but this soliton is different from that shown in Fig. 1 for repulsive interspecies interactions.

For a better understanding of the influence of repulsive interspecies interactions on solitons, we demonstrate the variations of interval between two solitons' centers ΔX, the peak density $\max|\psi_{+1}(x,t)|^2$, and the width of soliton $\langle R\rangle_{+1}$ in ψ_{+1} component in Figs. 3(c)–3(e), respectively. From Figs. 3(c)–3(e), we can see that the peak density and the width of soliton display periodic oscillation. All this verifies that soliton breather is created in ψ_{+1} component. It is also seen that when ΔX has a minimum (maximum) value, the soliton breather in ψ_{+1} component has a minimum (maximum) peak and a maximum (minimum) width. This phenomenon can be explained by the fact that when ΔX has a minimum value, the repulsive potentials of two solitons have maximum values, so soliton breathers have a minimum peak and a maximum width, and vice versa. Moreover, the cycle of the soliton breather is around 29 (see Figs. 3(d) and 3(e)).

These novel soliton breathers are different from those in Refs. [35] and [36]. They are formed by two factors: the trapping potential and interspecies interactions. The trapping potential makes the condensates localize in a small region and prevents the dissolution of condensates. In addition, the movement of soliton breather is caused by the displacement of trap center. Due to repulsive interspecies interactions, which cause the elastic collision of two solitons, solitons change their width and peak maximum periodically.

3.2. Three-component solutions

We illustrate the soliton breathers in three-component state. First, we describe the initialization of the system. We assume that the three components are initially loaded into three different traps of the same strength,[37] $V_j(x)$, centered at different positions,

$$V_j(x) = \frac{1}{2}(x - jx_0)^2, \quad j = -1, 0, +1. \tag{7}$$

Here, we choose the nonlinearity coefficients $c_0 = c_2 = c = -1.0$. The BECs fulfill the 1D GPEs as follows:

$$\begin{aligned} i\partial_t \psi_{+1} = & \left(-\frac{1}{2}\partial_x^2 + \frac{1}{2}(x - x_0)^2\right)\psi_{+1} \\ & + 2c\left(|\psi_{+1}|^2 + |\psi_0|^2\right)\psi_{+1} + c\psi_0^2\psi_{-1}^*, \end{aligned}$$

$$
\begin{aligned}
\mathrm{i}\partial_t \psi_0 &= \left(-\frac{1}{2}\partial_x^2 + \frac{1}{2}x^2\right)\psi_0 \\
&\quad + 2c\left(|\psi_{+1}|^2 + |\psi_{-1}|^2\right)\psi_0 + 2c\psi_{+1}\psi_0^*\psi_{-1}, \\
\mathrm{i}\partial_t \psi_{-1} &= \left(-\frac{1}{2}\partial_x^2 + \frac{1}{2}(x+x_0)^2\right)\psi_{-1} \\
&\quad + 2c\left(|\psi_{-1}|^2 + |\psi_0|^2\right)\psi_{-1} + c\psi_0^2\psi_{+1}^*. \qquad (8)
\end{aligned}
$$

We prepare the ground state of the system (8) with $x_0 = 1.0$ and $c = -1.0$ by using the imaginary time propagation method starting from the test wave function: $\psi_{+1}(x) = \psi_0(x) = \psi_{-1}(x) = \pi^{-1/4}\exp(-x^2/2)$. The densities $|\psi_j(x,t)|^2 (j = +1,0,-1)$ in the ground state are shown in Fig. 4.

After preparing this ground state, the three traps $V_j(x)(j = +1,0,-1)$ are suddenly changed into $V_j(x) = \frac{1}{2}x^2$ at $t = 0$. The time evolution of the three-component state is obtained by the time-splitting spectral method starting from its ground state, which is shown in Fig. 5.

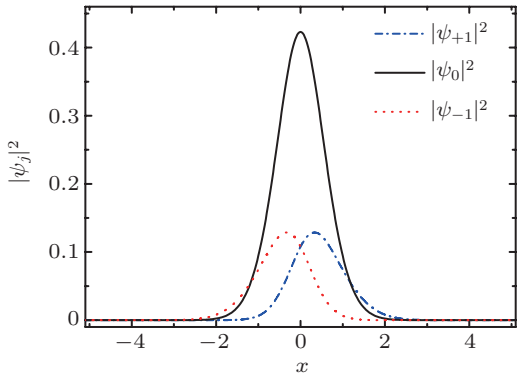


Fig. 4. Densities of the three components $\psi_j(j = +1,0,-1)$ in the ground state of system (8) with $x_0 = 1.0$ and $c = -1.0$. Here x and $|\psi_j|^2 (j = +1,0,-1)$ are measured in units of a_s and a_s^{-1}, respectively.

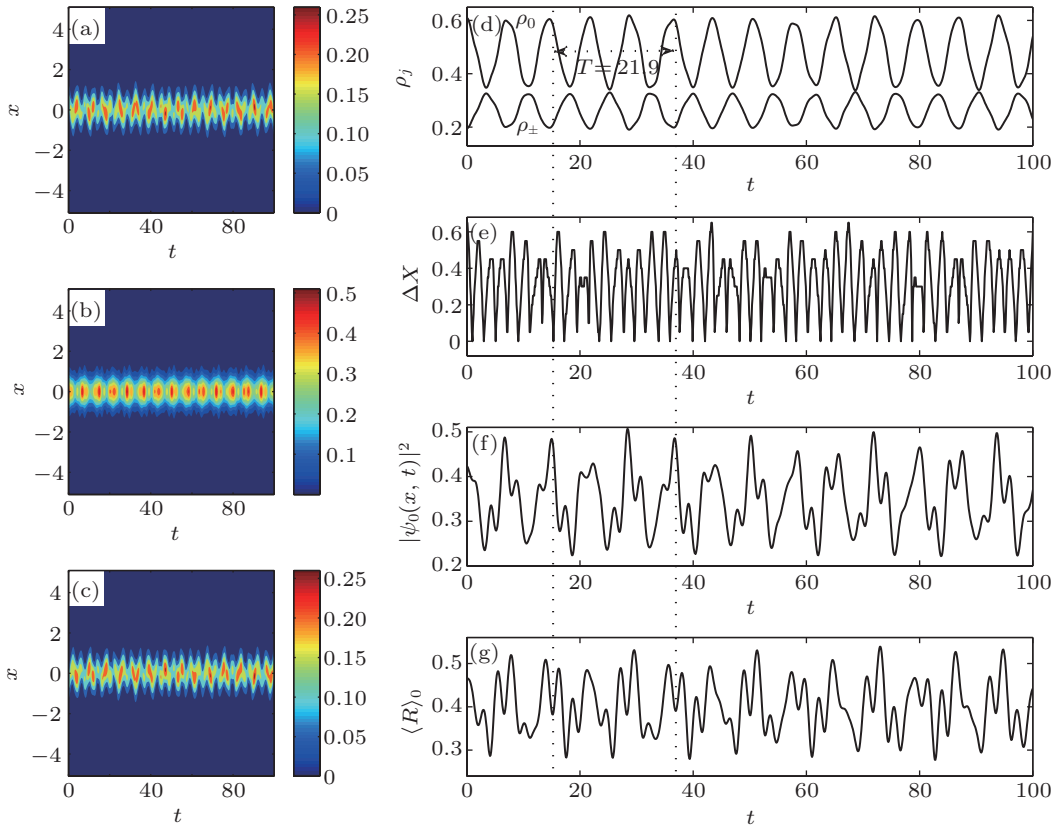


Fig. 5. (color online) After preparing the ground state of system (8) shown in Fig. 4, the three traps $V_j(x)(j = +1,0,-1)$ are suddenly changed into $V_j(x) = \frac{1}{2}x^2$ at $t = 0$. (a), (b), and (c) Spatiotemporal contour plot of the densities $|\psi_j(x,t)|^2$ in the components ψ_{+1}, ψ_0, and ψ_{-1}, respectively. (d) and (e) Time evolution of the relative densities ρ_j in three components $\psi_{\pm 1}$ (identical to each other, i.e., $\rho_{+1} = \rho_{-1}$) and ψ_0, ΔX (i.e., the interval between centers of the condensates in components $\psi_{\pm 1}$). (f) and (g) Time evolution of the peak density $|\psi_0(x = 0,t)|^2$ and the width $\langle R\rangle_0$ of condensates in the ψ_0 component, respectively. Here x, ΔX, and $\langle R\rangle_0$ are measured in units of a_s. The t and $|\psi_j|^2 (j = +1,-1)$ are measured in units of ω_x^{-1} and a_s^{-1}, respectively.

Figures 5(a)–5(c) show the time evolution of the densities $|\psi_j(x,t)|^2$ in three components ψ_{+1}, ψ_0, and ψ_{-1}, respectively. The soliton breathers are created in three components, which are periodic and different from those illustrated in Ref. [10]. Here we only focus on analyzing soliton breather generated in the ψ_0 component.

For a better understanding of the influence of attractive interspecies interactions and spin exchange collision on the soliton breather in the ψ_0 component, we plot Figs. 5(d)–5(g) to show the time dependence of the relative densities ρ_j

$(j=+1,0,-1)$ in three components, the interval between centers of the condensates in components $\psi_{\pm1}$ (i.e., ΔX), the peak density $|\psi_0(x=0,t)|^2$, and the width $\langle R\rangle_0$ of condensates in the ψ_0 component, respectively. From Fig. 5(d), we can see that spin populations display periodic oscillation caused by the spin exchange collision (atoms are periodically transferred from $\psi_{\pm1}$ components into ψ_0 component, and vice versa), which is similar to that illustrated in Refs. [10] and [13].

It is well known that spin exchange collision is coherent and it supports the existence of spinor solitons. As is shown in Figs. 5(f) and 5(g), we can see the peak density $|\psi_0(x=0,t)|^2$ and the width $\langle R\rangle_0$ of condensates in the ψ_0 component display periodic oscillation. When the peak density has a minimum (maximum) value, the width has a maximum (minimum) value. The peak density and the width have the same cycle. This verifies that soliton breather is generated in the ψ_0 component. From Figs. 5(d)–5(g), we can see that the cycle of this soliton breather is around 21.9. When ρ_0 has a minimum (maximum) value, the soliton breather in ψ_0 component has a minimum (maximum) peak density and a maximum (minimum) width. However, this soliton breather is different from that illustrated in Ref. [10]. The peak density $|\psi_0(x=0,t)|^2$ and the width $\langle R\rangle_0$ of soliton breather in the ψ_0 component have more complex periodic oscillation (see Figs. 5(f) and 5(g)), and the peak density of ψ_0 component is not directly proportional to its population (see Figs. 5(d) and 5(f)). These differences are caused by the collision of atoms in different components.

4. Conclusions

In this work, by numerically solving the 1D time-dependent coupled GPEs that describe the dynamics of spin-1 condensates, we demonstrate the collision of condensates in two-component and three-component states. In two-component state, we find three different scenarios: (i) the two condensates with no interspecies interactions make elastic collision and form stable bright solitons; (ii) the two condensates with attractive interspecies interactions make inelastic collision; (iii) the two condensates with repulsive interspecies interactions make elastic collision and form soliton breathers, the peak density and width of these soliton breathers are related to the interval between two solitons' centers. We also give explanations for these three different scenarios. In three-component state, we present novel soliton breathers in three components, and find the possible reasons for those soliton breathers. These findings suggest new possibilities in the study of spin-1 condensates.

References

[1] Stenger J, Inouye S, Stamper-Kurn D M, Miesner H J, Chikkatur A P and Ketterle W 1998 *Nature* **396** 345
[2] Miesner H J, Stamper-Kurn D M, Stenger J, Inouye S, Chikkatur A P and Ketterle W 1999 *Phys. Rev. Lett.* **82** 2228
[3] Chang M S, Qin Q, Zhang W, You L and Chapman M S 2005 *Nat. Phys.* **1** 111
[4] Ho T L 1998 *Phys. Rev. Lett.* **81** 742
[5] Ohmi T and Machida K 1998 *J. Phys. Soc. Jpn.* **67** 1822
[6] Choi J y, Kwon W J and Shin Y i 2012 *Phys. Rev. Lett.* **108** 035301
[7] Zhai H, Chen W Q, Xu Z and Chang L 2003 *Phys. Rev. A* **68** 043602
[8] Ieda J, Miyakawa T and Wadati M 2004 *Phys. Rev. Lett.* **93** 194102
[9] Ieda J, Miyakawa T and Wadati M 2004 *J. Phys. Soc. Jpn.* **73** 2996
[10] Li L, Li Z, Malomed B A, Mihalache D and Liu W M 2005 *Phys. Rev. A* **72** 033611
[11] Uchiyama M, Ieda J and Wadati M 2006 *J. Phys. Soc. Jpn.* **75** 064002
[12] Nistazakis H E, Frantzeskakis D J, Kevrekidis P G, Malomed B A and Carretero-González R 2008 *Phys. Rev. A* **77** 033612
[13] Dabrowska-Wüster B J, Ostrovskaya E A, Alexander T J and Kivshar Y S 2007 *Phys. Lett. A* **75** 023617
[14] Zhong W P, Belić M R, Lu Y and Huang T 2010 *Phys. Rev. E* **81** 011605
[15] Zhao L C and Liu J 2012 *J. Opt. Soc. Am. B* **29** 3119
[16] Inouye S, Andrews M R, Stenger J, Miesner H J, Stamper-Kurn D M and Ketterle W 1998 *Nature* **392** 151
[17] Cornish S L, Claussen N R, Roberts J L, Cornell E A and Wieman C E 2000 *Phys. Rev. Lett.* **85** 1795
[18] Donley E A, Claussen N R, Cornish S L, Roberts J L, Cornell E A and Wieman C E 2001 *Nature* **412** 295
[19] Zhao L C and Liu J 2013 *Phys. Rev. E* **87** 013201
[20] Strecker K E, Partridge G B, Truscott A G and Hulet R G 2002 *Nature* **417** 150
[21] Cornish S L, Thompson S T and Wieman C E 2006 *Phys. Rev. Lett.* **96** 170401
[22] Abdullaev F Kh, Kamchatnov A M, Konotop V V and Brazhnyi V A 2003 *Phys. Rev. Lett.* **90** 230402
[23] Wang Y S, Yan P G, Li B and Liu X S 2012 *Chin. Phys. B* **21** 010309
[24] Yan P G, Wang Y S, Ji S T and Liu X S 2012 *Phys. Lett. A* **376** 3141
[25] Yan P G, Ji S T and Liu X S 2013 *Phys. Lett. A* **377** 878
[26] Kevrekidis P G, Theocharis G, Frantzeskakis D J and Malomed B A 2003 *Phys. Rev. Lett.* **90** 230401
[27] Zhang X F, Hu X H, Liu X X and Liu W M 2009 *Phys. Rev. A* **79** 033630
[28] Matuszewski M, Alexander T J and Kivshar Y S 2009 *Phys. Rev. A* **80** 012602
[29] Song S W, Wang D S, Wang H and Liu W M 2012 *Phys. Rev. A* **85** 063617
[30] Hai W, Lee C and Chong G 2004 *Phys. Rev. A* **70** 053621
[31] Matuszewski M 2010 *Phys. Rev. A* **82** 053630
[32] Bao W, Jaksch D and Markovich P A 2003 *J. Comput. Phys.* **187** 318
[33] Bao W and Zhang Y 2005 *Math. Models Meth. Appl. Sci.* **15** 1863
[34] Hua W, Li B and Liu X S 2011 *Chin. Phys. B* **20** 060308
[35] Zhao L C, Yang Z Y, Ling L M and Liu J 2011 *Phys. Lett. A* **375** 1839
[36] Baronio F, Degasperis A, Conforti M and Wabnitz S 2012 *Phys. Rev. Lett.* **109** 044102
[37] Nistazakis H E, Frantzeskakis D J, Kevrekidis P G, Malomed B A, Carretero-González R and Bishop A R 2007 *Phys. Rev. A* **76** 063603